



University of Groningen

Rheological behavior of precursor PPV monolayers

Luinge, JW; Nijboer, GW; Hagting, JG; Vorenkamp, EJ; Fuller, GG; Schouten, AJ

Published in:
Langmuir

DOI:
[10.1021/la048234+](https://doi.org/10.1021/la048234+)

IMPORTANT NOTE: You are advised to consult the publisher's version (publisher's PDF) if you wish to cite from it. Please check the document version below.

Document Version
Publisher's PDF, also known as Version of record

Publication date:
2004

[Link to publication in University of Groningen/UMCG research database](#)

Citation for published version (APA):

Luinge, JW., Nijboer, GW., Hagting, JG., Vorenkamp, EJ., Fuller, GG., & Schouten, AJ. (2004). Rheological behavior of precursor PPV monolayers. *Langmuir*, 20(26), 11517-11522. <https://doi.org/10.1021/la048234+>

Copyright

Other than for strictly personal use, it is not permitted to download or to forward/distribute the text or part of it without the consent of the author(s) and/or copyright holder(s), unless the work is under an open content license (like Creative Commons).

Take-down policy

If you believe that this document breaches copyright please contact us providing details, and we will remove access to the work immediately and investigate your claim.

Downloaded from the University of Groningen/UMCG research database (Pure): <http://www.rug.nl/research/portal>. For technical reasons the number of authors shown on this cover page is limited to 10 maximum.

Rheological Behavior of Precursor PPV Monolayers

J. W. Luinge,^{*,†} G. W. Nijboer,[†] J. G. Hagting,[†] E. J. Vorenkamp,[†]
G. G. Fuller,[‡] and A. J. Schouten[†]

Department of Polymer Chemistry and Materials Science Centre, University of Groningen,
Nijenborgh 4, 9747 AG Groningen, The Netherlands, and Department of Chemical
Engineering, Stanford University, Stanford, California 94305-5025

Received July 14, 2004. In Final Form: September 27, 2004

The rheological behavior of different precursor poly(*p*-phenylene vinylene) (prec-PPV) monolayers at the air–water interface was investigated using an interfacial stress rheometer (ISR). This device nicely reveals a transition of the precursor poly(2,5-dimethoxy-1,4-phenylene vinylene) (prec-DMePPV) monolayer from Newtonian to elastic behavior with increasing surface pressure. The transition is accompanied by an increase in the modulus. This behavior coincides with the coagulation of different 2D condensed domains as revealed by Brewster angle microscopy (BAM). However, partly converted prec-DMePPV monolayers show elastic behavior even at low surface pressures, although a sudden increase of the moduli does occur. This phenomenon is attributed to enhanced hydrophobic interactions between the conjugated moieties in the partly converted polymers. The latter also explains the stretching behavior of the partly converted prec-DMePPV upon transfer in Langmuir–Blodgett-type vertical dipping. The increase of the moduli which is observed is much more gradual in the precursor poly(2,5-dibutoxy-1,4-phenylene vinylene), prec-DBuPPV, a monolayer which is in agreement with the expected expanded state of the latter monolayer.

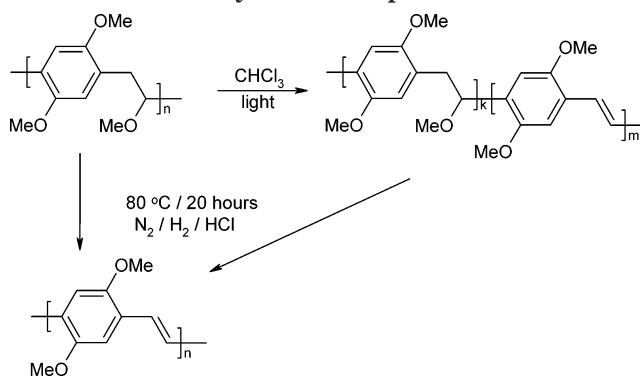
Introduction

Poly(*p*-phenylene vinylene) polymers exhibit interesting features due to their π -conjugation, which makes them well-known candidates for several optoelectronic devices. A suitable technique for the assembly of these devices is via a layer-by-layer deposition.^{1,2} In this way, the Langmuir–Blodgett technique offers the possibility of combining different alternating monolayers. To obtain stable monolayers of PPVs, a precursor PPV is spread at the air–water interface, deposited on a substrate, and subsequently converted to the corresponding PPV polymer,³ see Scheme 1.

The conformation of PPV precursor polymers, and many other flexible polymers, at the air–water interface can be considered either as 2D collapsed coils or as 2D expanded coils. Whether a molecule is in one of these states depends on the interaction balance between internal cohesive forces and polymer–water “adhesive” forces. Temperature, constituents, and main-chain rotation potentials play an important role in this behavior.⁴

It is difficult to imagine two different chains at the air–water interface in an “entangled” state such as in 3D. It is even predicted that entanglements in 2D do not exist, even in the expanded state, although simulations show that there can be considerable interpenetration.^{5,6} Together, this produces a picture of the monolayer in which the chains are 2D curled up individually and aggregate together in flat molecularly thick plates. The interaction

Scheme 1. Conversion of prec-DMePPV to DMePPV via Partly Converted pc-DMePPV



within these plates, and thus between the molecules, is of the same order as the intramolecular cohesive interactions. In the case of PPV precursors, it has been found before⁷ that the segment orientation with respect to the interface was, on average, almost perpendicular, and therefore we assume the π – π interactions dominate in this case. Only with the dibutoxy-substituted precursor was an expanded state formed, in which case it was assumed that the segmental orientation was parallel to the interface. It can be expected that different intersegmental cohesive interactions will result in clearly different rheological behavior of the corresponding monolayers.

Moreover, when chain segment sequences have converted into a semiconducting π -conjugated form, it is foreseen that these elements will exhibit much stronger π – π stacking interactions which connect different chains more tightly than in the case of pure precursor polymers. In the extreme case, these interactions can be considered as intra- and intermolecular cross-links. It was observed in earlier studies that these cross-links give rise to molecular orientation in the monolayers on the substrate,

(7) Hagting, J. G.; Vorenkamp, E. J.; Schouten, A. J. *Macromolecules* **1999**, 32, 6619–6625.

* Corresponding author. E-mail: j.w.luinge@chem.rug.nl.

[†] University of Groningen.

[‡] Stanford University.

(1) Fou, A. C.; Onitsuka, O.; Ferreira, M.; Rubner, M. F.; Hsieh, B. R. *J. Appl. Phys.* **1996**, 79, 7501–7509.

(2) Hagting, J. G.; de Vos, R. E. T. P.; Sinkovics, K.; Vorenkamp, E. J.; Schouten, A. J. *Macromolecules* **1999**, 32, 3939–3945.

(3) Hagting, J. G.; de Vos, R. E. T. P.; Sinkovics, K.; Vorenkamp, E. J.; Schouten, A. J. *Macromolecules* **1999**, 32, 3930–3938.

(4) Brinkhuis, R. H. G.; Schouten, A. J. *Langmuir* **1992**, 8, 2247–2254.

(5) Yethiraj, A. *Macromolecules* **2003**, 36, 5854–5862.

(6) Ostrovsky, B.; Smith, M. A.; BarYam, Y. *Int. J. Mod. Phys. C* **1997**, 8, 931–939.

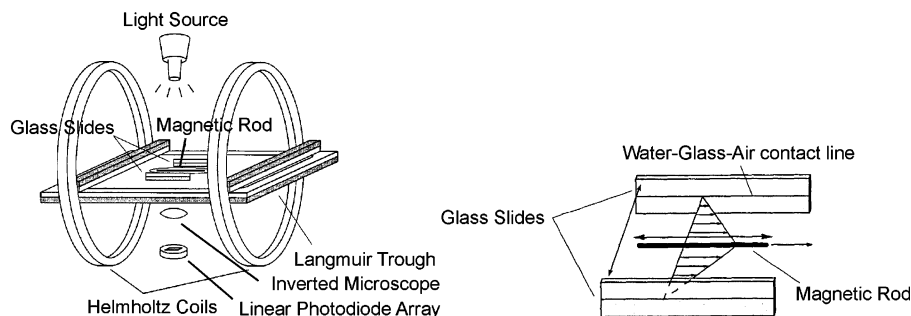


Figure 1. Schematic representation of the interfacial stress rheometer. A magnetic rod that resides on the air–water interface is oscillated by two magnetic coils. The oscillation is recorded via a linear photodiode array.

a phenomenon that was observed formerly only by employing rigid rods.^{8–10} Orientation in the current direction is desirable for the optoelectronic efficiency of the assembly.^{11–15}

It was observed that the alignment was obtained during the upstroke of partly converted prec-DMePPV monolayers.^{16,17} It was assumed partly converted prec-DMePPV (pc-DMePPV) monolayers form a 2D physical network at the air–water interface due to enhanced hydrophobic interactions of the conjugated moieties. During the upstroke of the transfer process, the physical network is stretched, giving rise to molecular orientation on the substrates, which is referred to as drawing behavior.

In this study, the rheological behaviors of monolayers of prec-DMePPV and 10% pc-DMePPV were compared to verify these results using an interfacial stress rheometer (ISR) and Brewster angle microscopy (BAM). The ISR has proved to be a successful device for the determination of the rheological behavior of monolayers at the air–water interface,^{18,19} and thus for the detection of a 2D (physical) network.²⁰ Furthermore, the rheological behavior of monolayers of prec-DBuPPV was investigated, which, due to their longer alkyl side chains, show an interesting peculiar behavior.

For these measurements, a magnetic rod, floating at the air–water interface, is oscillated by an oscillating magnetic field. The position of the rod is determined by a photodiode array. The moduli of the monolayer are calculated by comparing the master oscillation of the magnetic coils with the oscillation of the rod. A schematic representation of the ISR is given in Figure 1.

Experimental Section

The synthesis of prec-DMePPV, pc-DMePPV, and prec-DBuPPV has been described earlier.³ It was determined by GPC that the average molecular weights of the precursor PPVs were

(8) Kim, J.; McHugh, S. K.; Swager, T. M. *Macromolecules* **1999**, *32*, 1500–1507.

(9) Wu, Z. K.; Wu, S. X.; Liang, Y. Q. *Synth. Met.* **2002**, *130*, 35–38.

(10) Wu, Z. K.; Wu, S. X.; Liang, Y. Q. *Spectrochim. Acta, Part A* **2003**, *59*, 1631–1641.

(11) Tanigaki, N.; Kyotani, H.; Wada, M.; Kaito, A.; Yoshida, Y.; Han, E.-M.; Abe, K.; Yase, K. *Thin Solid Films* **1998**, *331*, 229–238.

(12) Stengersmith, J. D.; Lenz, R. W.; Wegner, G. *Makromol. Chem., Macromol. Chem. Phys.* **1989**, *190*, 3005–3011.

(13) Gagnon, D. R.; Karasz, F. E.; Thomas, E. L.; Lenz, R. W. *Synth. Met.* **1987**, *20*, 85–95.

(14) Liang, W.; Karasz, F. E. *Polymer* **1991**, *32*, 2363–2366.

(15) Kemerink, M.; Van Duren, J. K. J.; Jonkheijm, P.; Pasveer, W. F.; Koenraad, P. M.; Janssen, R. A. J.; Salemink, H. W. M.; Wolter, J. H. *Nano Lett.* **2003**, *3*, 1191–1196.

(16) Hagting, J. G.; Vorenkamp, E.; Schouten, A. J. *Thin Solid Films* **1998**, *329*, 65–68.

(17) Hagting, J. G.; Schouten, A. J. *Langmuir* **2000**, *16*, 4348–4351.

(18) Brooks, C. F.; Fuller, G. G.; Frank, C. W.; Robertson, C. R. *Langmuir* **1999**, *15*, 2450–2459.

(19) Anseth, J. W.; Bialek, A.; Hill, R. M.; Fuller, G. G. *Langmuir* **2003**, *19*, 6349–6356.

(20) Yim, K. S.; Rahaii, B.; Fuller, G. G. *Langmuir* **2002**, *18*, 6597–6601.

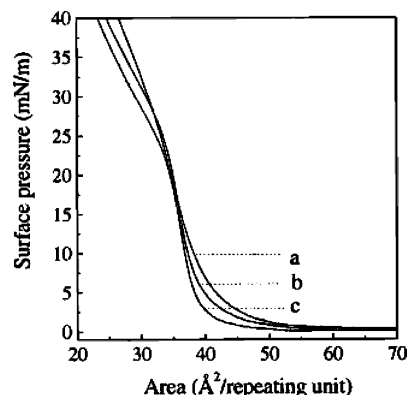


Figure 2. Surface pressure isotherms of partly converted pc-DMePPV: (a) 0% conversion, (b) 10% conversion, and (c) 20% conversion. $T = 15^\circ\text{C}$.

rather high ($M_n \approx 1 \times 10^6$, $M_w \approx 3 \times 10^5$ g/mol). It was found that partial conversion results in a decrease of the number average molecular weight to 2×10^4 g/mol.

Polymer solutions of about 0.2 mg/mL in CHCl_3 , containing one drop of pyridine in 10 mL of solution, to prevent the polymer from oxidizing, were spread at the air–water interface. All experiments performed with 10% pc-DMePPV were carried out under an inert argon atmosphere to prevent interfacial oxidation.¹⁷ The Teflon trough (33.0×7.5 cm) was supplied by KSV Instruments and was equipped with a quartz window flush in the bottom of the trough. Two hydrophobic barriers were moved symmetrically to change the surface pressure of the monolayer at the air–water interface. The surface pressure was monitored by a Wilhelmy balance, and all experiments were carried out at 15°C . All measurements were performed at a compression speed of 5 \AA per repeating unit per minute, unless otherwise stated. BAM was performed using p-polarized light from a 10 mW argon laser beam set to an angle of 53.1° to the air–water interface. A 50 mm planoconvex lens magnifies the reflected light from the monolayer, and the contrast was enhanced by the use of an analyzer. A more detailed description has been given earlier.¹⁸ Afterward, the contrast as well as the brightness of the photos were increased by 50%.

Results and Discussion

Comparison of isotherms of prec-DMePPV and pc-DMePPV led us to the belief that pc-DMePPV forms a more closely packed condensed monolayer due to enhanced hydrophobic interactions.⁷ Figure 2 depicts these isotherms in which it is shown that increasing conversion leads to a more compact monolayer. It was confirmed in this previous study that, upon spreading the polymer solution at the concentrations used, no crossovers were formed.³ Moreover, it was observed that compression speed had almost no influence on the position of the isotherms. Therefore, it was concluded that no pressure gradient builds up during compression. Decreasing the area to

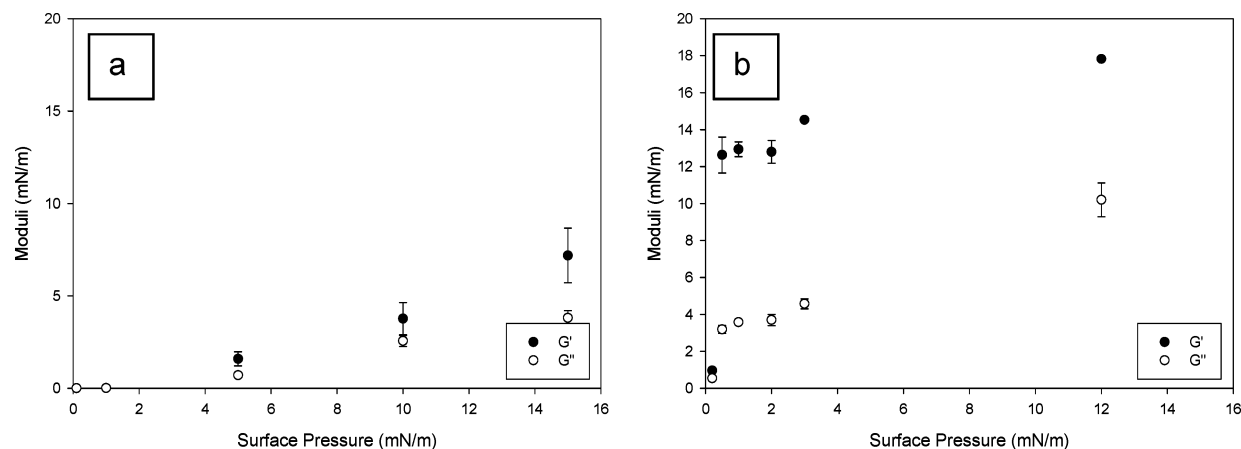


Figure 3. Moduli of (a) prec-DMePPV and (b) 10% pc-DMePPV versus surface pressure. $\nu = 0.15$ rad/s, $\epsilon = 0.02$.

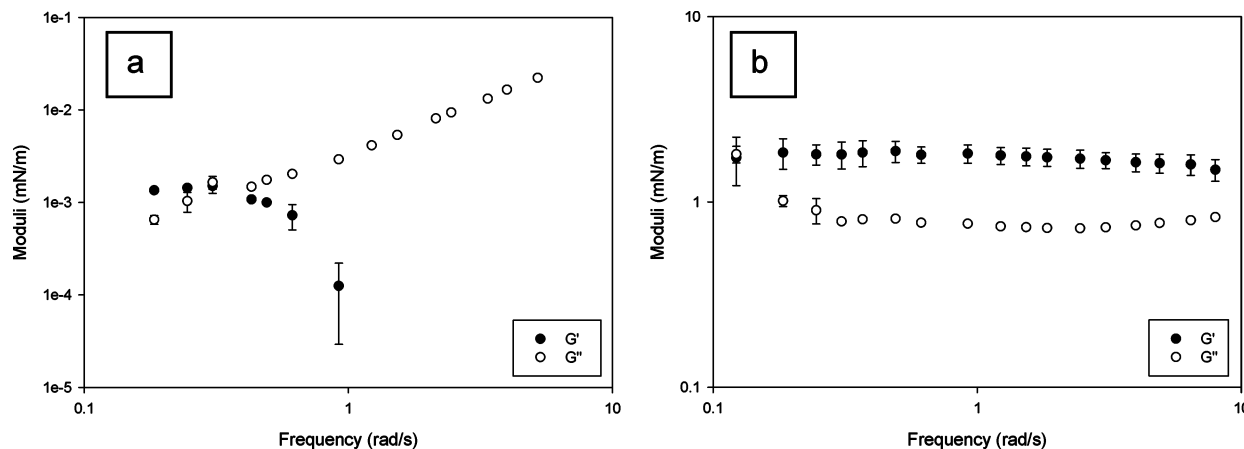


Figure 4. Dependence of the moduli of prec-DMePPV monolayers on the frequency at different surface pressures, $\epsilon = 0.02$: (a) 0.1 mN/m; (b) 5 mN/m.

around $35 \text{ \AA}^2/\text{repeating unit}$ resulted in (partial) collapse of the monolayer and formation of double layers.

The rheological behavior of these monolayers is depicted in Figure 3. Figure 3a shows the storage modulus G' , and the loss modulus G'' , of a prec-DMePPV monolayer as a function of surface pressure. At low surface pressures, both G' and G'' are negligible. Increasing the surface pressure results in a rather strong increase of the moduli. Moreover, the value of G' exceeds G'' , meaning that a more elastic monolayer is obtained. This is explained by an increase in interactions between the 2D condensed plates upon increasing the surface pressure.

In contrast to prec-DMePPV, 10% pc-DMePPV shows a sudden rise of the storage and loss modulus. Interestingly, the value of G' exceeds G'' , even at low surface pressures. This means that the monolayer behaves elastic even in this regime. It was also noticed that the moduli at low surface pressures are much higher than in the case of prec-DMePPV. An exceedingly stiff monolayer was obtained by spreading 20% pc-DMePPV on the air–water interface. Quantitative results, however, could not be obtained due to its enormous stiffness, which was beyond the measuring capacity of the equipment. The elastic behavior of 10% pc-DMePPV monolayers can be explained by the enhanced hydrophobic interactions between the 2D condensed plates, resulting in a 2D physical network even at very low surface pressures. The enormous increase of the moduli upon converting prec-DMePPV confirms the increase of the interactions in the monolayer. The hydrophobic interactions in pc-DMePPV can be treated as physical cross-links. The stronger interactions give rise

to a more tenacious network. The increase in elasticity is indicated by the increase of the ratio between G'' and G' , $\tan \delta$. This also explains the drawing behavior that was observed upon transfer of the pc-DMePPV monolayer to substrates in earlier studies and which is discussed in the Introduction. It is believed these extra interactions are responsible for the relaxation of the monolayer at the air–water interface and the molecular orientation of the pc-DMePPV chains on the substrate during the transfer process.

Returning to the rheological behavior of prec-DMePPV monolayers, Figure 4 depicts the frequency-dependent behavior of these monolayers, in which G' and G'' are measured as a function of frequency at different surface pressures. From these figures, we see Newtonian behavior for surface pressure lower than 0.2 mN/m. The moduli are very low; at higher surface pressures, an elastic monolayer is observed. At this and higher surface pressures, the surface moduli are only slightly dependent on the frequency, typical for cross-linked systems. This means a transition from Newtonian to a more rubberlike behavior takes place. An explanation for this transition can be found in the BAM pictures, shown in Figure 5. The images of the monolayer at the air–water interface show separate domains above $70 \text{ \AA}^2/\text{repeating unit}$. These results confirm the suggested 2D-condensed domains of prec-DMePPV mentioned earlier and resemble the domains in similar polythiophene monolayers.²¹ Below this area, around 67

(21) Greve, D. R.; Dynarowicz-Latka, P.; Dhanabalan, A.; Janssen, R. A. J. *Colloids Surf., A* **2002**, 198–200, 323–330.

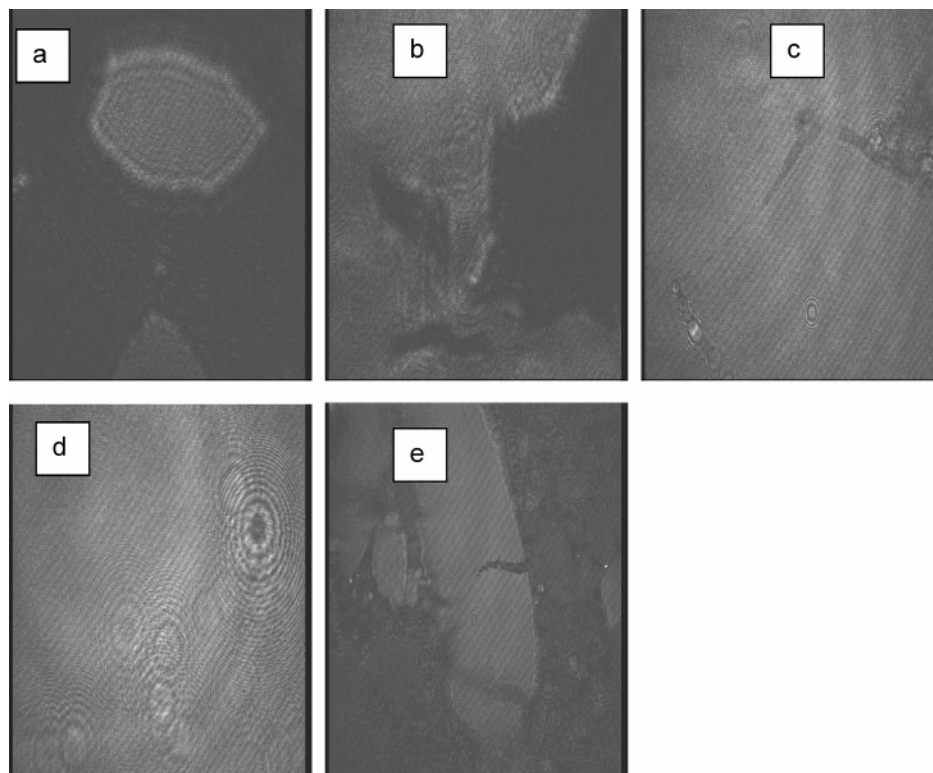


Figure 5. Brewster angle microscopy pictures taken of a prec-DMePPV monolayer at the air–water interface during compression at (a) 99, (b) 67, (c) 41, (d) 26 Å²/rep unit and subsequent expansion, and (e) 39 Å²/rep unit.

Å²/repeating unit, the different plates start to touch each other. It was observed that at an area of 60 Å²/repeating unit the flowing plates become fixed, which coincides nicely with the area at which the surface pressure starts to increase. Further reducing the surface area causes an increasing packing density, reducing the amount of holes between the platelets, shown in Figure 5c. At this point, the isotherm of the prec-DMePPV monolayer shows a rapid increase, accompanied by a rise of the moduli as a function of the surface pressure. Figure 5d shows that decreasing the surface area further gives rise to a homogeneous monolayer. Subsequent expansion of the monolayer results in breakage into separate plates, and a monolayer similar to the starting conditions is obtained, depicted in Figure 5e. In summary, at low surface pressure, both moduli are determined by the separate floating domains, leading to Newtonian behavior, whereas upon increasing the surface pressure, an increasing amount of interactions between the domains occurs, leading to elastic behavior and an increasingly stiffer monolayer.

Figure 6 depicts the results of several creep experiments on prec-DMePPV monolayers, to further elucidate the structure of the prec-DMePPV monolayer. For these creep measurements, the displacement of the magnetic rod as a result of the application of a constant magnetic field and, subsequently, the movement due to relaxation after removing this field are measured.

Figure 6a shows that, upon application and subsequent removal, a viscoelastic behavior of the prec-DMePPV monolayer is observed, of which the elastic recovery is around 40%. Upon increasing the surface pressure, more stress is needed to bring about any detectable movement of the rod. The deflection of the rod is, however, a lot smaller. In addition, the elastic recovery is now increased to 60%. The increase in elasticity can be explained by an increased network formation due to enhanced hydrophobic interactions. Figure 6c depicts the creep behavior at 15

mN/m. The stress applied is equal to Figure 6b; however, this increase in surface pressure results in viscous flow, with only a very small elastic part. This flow is even more pronounced in Figure 6d, in which, again, the stress is increased, and the elastic part is decreased. A possible explanation for the difference between the results depicted in Figure 6b and 6c,d might be the following. First, upon compression of the monolayer, the free volume between the chains is reduced. It can be seen from the isotherm, depicted in Figure 2, that at 15 mN/m the monolayer is almost in its most condensed state. It is known that reduction of free volume results in more brittle behavior.²² Because of this reduction in free volume, the monolayer is not able to delocalize the stress induced by the rod, resulting in brittle fracture and subsequently in viscous flow. It has to be noted from Figure 3a that in this regime no significant change in the difference of G' and G'' is found. This implies that the amount of hydrophobic interactions, acting as cross-links, is almost equal and can only have a minor effect on the brittle behavior of the monolayer, which is in accordance with literature.²³

It would be interesting to compare the creep behavior of monolayers of prec-DMePPV with 10% pc-DMePPV. Unfortunately, it proved to be very difficult to measure this behavior of 10% pc-DMePPV, due to the high stiffness of these monolayers.

The rheological behavior of a prec-DMePPV monolayer is in sharp contrast with the behavior of prec-DBuPPV. This is in accordance with the model of a 2D expanded state of the prec-DBuPPV proposed earlier.³ Figure 7a depicts isotherms of a prec-DBuPPV monolayer at different temperatures; the different transitions, calculated by MM2 force field minimizations,² are schematically

(22) Hill, A. J.; Zipper, M. D.; Tant, M. R.; Stack, G. M.; Jordand, T. C.; Schultz, A. R. *J. Phys.: Condens. Matter* **1996**, *8*, 3811–3827.

(23) Smit, R. J. M.; Berkelmans, W. A. M.; Meijer, H. E. H. *J. Mater. Sci.* **2000**, *35*, 2855–2867.

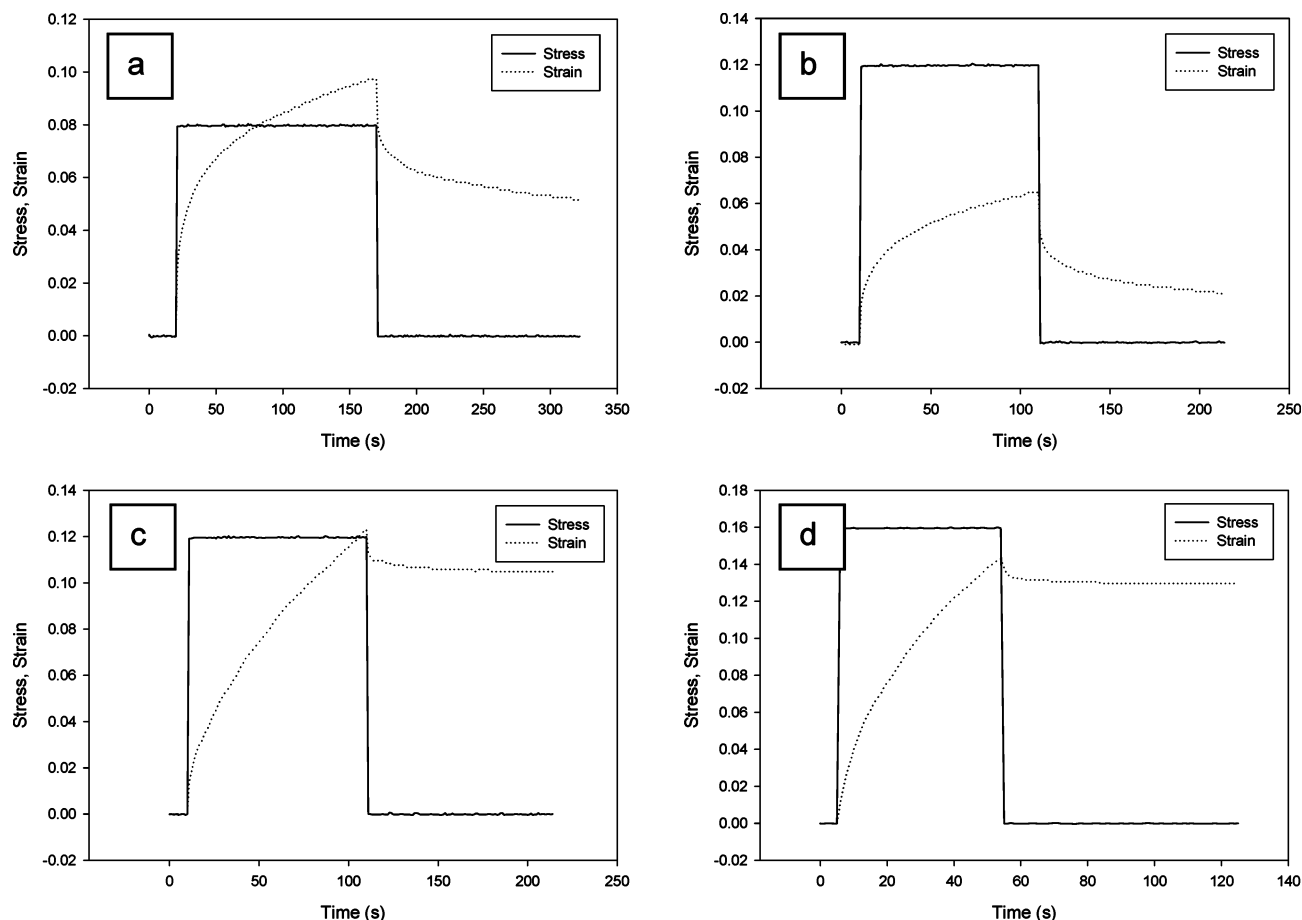


Figure 6. Stress-strain curves of prec-DMePPV monolayer at different surface pressures: (a) 5 mN/m, (b) 10 mN/m, (c) 15 mN/m, and (d) 20 mN/m.

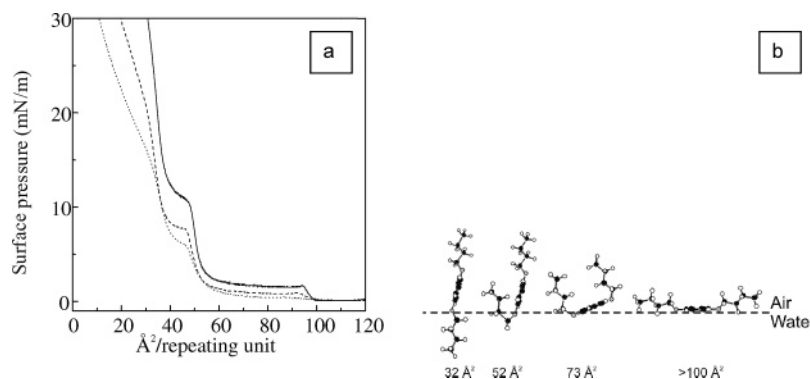


Figure 7. (a) Influence of temperature on the pressure-area isotherm of prec-DBuPPV. Temperature: 10 °C (—), 21 °C (---), and 38 °C (····). (b) Side view of the conformations of the aromatic ring of prec-DBuPPV, area per repeating unit: >100 , 73, 52, and 32 \AA^2 . Carbon, black atoms; oxygen, gray atoms; hydrogen, white atoms.

represented in Figure 7b. The structural changes of prec-DBuPPV that are depicted in this figure were confirmed with IR spectroscopy of this polymer at the air-water interface.³ It was seen that the intensity of the carbonyl peak, which lies in the plane of the phenylene ring, became relatively small with decreasing surface areas, indicating a perpendicular orientation to the air-water interface. Figure 7b shows that compression of the monolayer to around 93 $\text{\AA}^2/\text{repeating unit}$ results in perpendicular orientation of the butoxy moieties, which explains the first transition in the isotherms. Further compression to around 52 $\text{\AA}^2/\text{repeating unit}$ leads to perpendicular orientation of the phenylene ring to the air-water interface. At even lower surface areas, one butoxy moiety is pushed into the water layer. Collapse of the monolayer is in this case

slightly dependent on temperature; however, it was found that monolayers showed (partial) collapse around 25 $\text{\AA}^2/\text{repeating unit}$.

The expanded state of the prec-DBuPPV is confirmed by BAM images shown in Figure 8. It can be concluded from these figures that prec-DBuPPV spreads homogeneously over the whole air-water interface. Except for Figure 8e, no domains are visible; this means that Figure 8a-d shows a plain gray area in which no transitions can be observed. Furthermore, it can be seen that the reflected light gradually increases with a decreasing area, see Figure 8a-c successively. This indicates a homogeneous increase in density of the chains at the air-water interface. It was observed that at surface areas below 60 $\text{\AA}^2/\text{repeating unit}$, the movement of occasional dust particles was

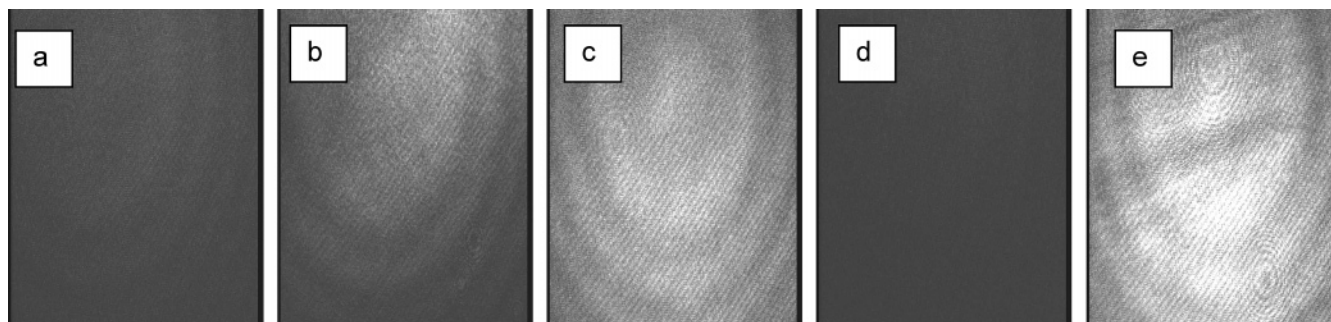


Figure 8. Brewster angle microscopy pictures taken of a prec-DBuPPV monolayer at the air–water interface at (a) 93, (b) 49, (c) 41, (d) 82, and (e) 29 Å²/rep unit.

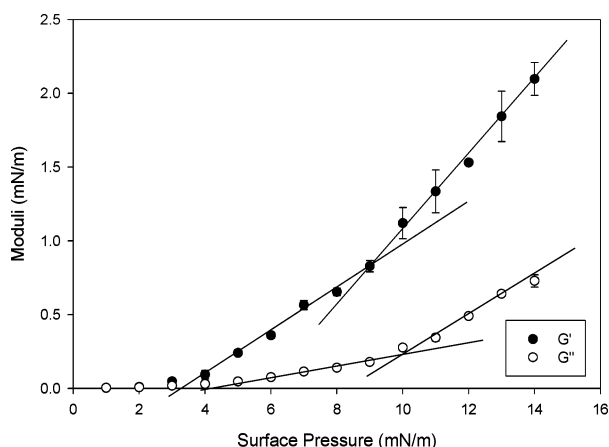


Figure 9. Moduli of a prec-DBuPPV monolayer at the air–water interface at different surface pressures. $\nu = 0.15$ rad/s, $\epsilon = 0.02$. Lines are linear best fits from 4 to 10 mN/m and 10 to 14 mN/m, respectively.

drastically hindered. This coincides with the second transition in the isotherm in which the phenylene rings are starting to orient perpendicular to the air–water interface.

Further decrease of the area to 41 Å²/repeating unit, followed by an increase of the area, shows that the process is fully reversible. Figure 8c and d depicts this behavior. The small brightness differences in Figure 8e suggest that compression to 29 Å²/repeating unit gives rise to double layers, as was also observed in Figure 7a.

Figure 9 depicts the rheological behavior of a prec-DBuPPV monolayer. Again, at low surface pressures, G' and G'' are negligible, but, instead of a sudden change in moduli, two different regimes can be distinguished. Up to 10 mN/m, the monolayer becomes increasingly elastic due to van der Waals interactions between the butoxy moieties, or as a result of the increasing penetration of the polymer chains, as mentioned in the Introduction.^{5,6} After the

phenylene rings are oriented perpendicular to the air–water interface and the butoxy moieties point out of the water phase, steric interactions between the butoxy moieties decrease. However, π – π interactions between the parallel oriented phenylene rings increase, and consequently phenylene rings approach each other, leading to enhanced hydrophobic interactions, resulting in a more stiff physical network. This leads to an increased slope of the moduli versus surface pressure. At these surface pressures, the moduli of prec-DBuPPV approach the moduli of the prec-DMePPV monolayer, corresponding to the similar, perpendicular, orientation of the phenylene rings at the air–water interface for both monolayers. The deviation results from the disruption of the stacking of the phenylene rings due to the free volume claimed by the butoxy moieties. This behavior is in good agreement with the 2D expanded state of the prec-DBuPPV monolayer suggested earlier and depicted in the isotherm shown in Figure 7.

Conclusion

In this study, BAM reveals a condensed domain structure of prec-DMePPV monolayers at low surface pressures accompanied by Newtonian behavior. At the moment the monolayer becomes continuous, a crossover of the loss and storage moduli occurs. Partly converted DMePPV monolayers show a more sudden increase of the moduli than monolayers of prec-DMePPV. However, interestingly, even below this increase the monolayer behaves as elastic, indicating that a 2D physical network is formed, caused by enhanced hydrophobic interactions between the longer conjugated moieties. The latter agrees well with the drawing behavior observed upon dipping. This increase of G' and G'' is more gradual in the case of prec-DBuPPV monolayers, in correspondence with the expected expanded state of the monolayer and butoxy side-group interactions.

LA048234+